

Preparation of a ZnO/TiO₂ vertical-nanoneedle-on-film heterojunction and its photocatalytic properties

Cite this: *RSC Adv.*, 2014, 4, 18186

Delong Li,^a Yupeng Zhang,^a Wenhui Wu^a and Chunxu Pan^{*ab}

This paper introduces a process to prepare a novel ZnO/TiO₂ heterojunction composite with ZnO nanoneedles vertically grown on a TiO₂ film *via* micro-arc oxidation (MAO), pulse plating and thermal oxidation. Firstly a TiO₂ thin film was prepared on a titanium substrate using MAO; then a Zn nanocrystalline film was pulse plated on the MAO film; finally the composite film was thermally treated at 380° for several hours, which transformed the Zn film into ZnO nanoneedles. SEM observations revealed that the ZnO nanoneedles were vertically grown on the TiO₂ film. The advantage of the ZnO/TiO₂ heterojunction was that during heat treatment, in addition to the phase transformation from Zn into ZnO, simultaneous short-range atom diffusion occurred at the interface between the ZnO nanoneedles and the TiO₂ layer, which encouraged the formation of a highly efficient, strong and stable heterojunction. Photocatalytic experiments demonstrated that, compared with pure ZnO or TiO₂, the as-prepared ZnO/TiO₂ composites showed greater efficiency and stability in photogenerated carriers and a significantly improved photocatalytic performance, due to this special heterojunction structure.

Received 3rd January 2014
Accepted 24th February 2014

DOI: 10.1039/c4ra00031e

www.rsc.org/advances

1. Introduction

Titanium dioxide (TiO₂) has attracted wide attention in the fields of photocatalysis and solar cells, due to its excellent optical and electronic properties, stability and security.¹ However, its applications are still limited because of its inherent defects involving a large band gap (anatase 3.2 eV), which restricts the absorbing wavelength to no longer than 387 nm within the UV light, and also the high recombining ratio of photo-induced electron-holes, which lowers its photocatalytic efficiency.^{1,2} Up to now, many methods have been proposed for overcoming these disadvantages; for example, doping with metal/non-metal ions³⁻⁵ and coupling with other oxide semiconductors.⁶⁻¹⁰ In general, coupling with an oxide semiconductor is a simple and efficient method to improve the photocatalytic efficiency.

After years of research, many composite systems have been reported, such as V₂O₅/TiO₂,⁶ SnO₂/TiO₂,⁷ CdO/TiO₂,⁸ and ZnO/TiO₂.¹¹⁻¹⁸ Of these, the ZnO/TiO₂ system has attracted the most attention.^{11,12} As a typical oxide semiconductor with a wide band gap, nano-sized ZnO has significant size effects and remarkable catalytic, optical and electronic properties, and has been widely used in applications including catalysts, optical and electronic devices and solar cells.¹⁹⁻²¹ Up to now, many methods have been

applied to prepare ZnO/TiO₂ composites, such as electrospinning,¹⁴ hydrothermal methods,^{13,15,16} and metal organic chemical vapor deposition (MOCVD),¹⁷ *etc.*

In general, the ZnO/TiO₂ composite can exhibit various morphologies, including nanofibers,¹¹⁻¹³ nanotubes,²⁹ nanoparticles,³⁰ and nano-films,³¹⁻³⁵ *etc.* Among the nano-film composite variant, different ways of combining the ZnO and the TiO₂ have been reported. For example, Kim *et al.*³¹ firstly prepared the ZnO and TiO₂ nanoparticles with a hydrothermal method, and then made them into a composite film of approximately 20 nm using sol-gel spin coating. Zhang *et al.*³² prepared a ZnO/TiO₂ composite film *via* vacuum evaporation and sol-gel methods, which resulted in a morphology of many particles on the surface of the film. Zhao *et al.*³³ introduced a process to prepare TiO₂ nanorods on a ZnO thin film, which was deposited upon a quartz substrate by epitaxial growth technology. Here, it was found that the TiO₂ nanorods grew along the ⟨001⟩ direction and reached 450 nm in length. Tian *et al.*³⁴ prepared a ZnO/TiO₂ film *via* a sol-gel process, and SEM observation revealed that the particles on the film surface were gradually reduced with a reduction of the Ti content. Mane *et al.*³⁵ prepared a ZnO/TiO₂ film on conductive glass by using chemical bath deposition, and found that the composite film was composed of many closely packed particles.

In fact, in a ZnO/TiO₂ composite system, its performance improvement, stability and service life are crucially determined by whether a heterojunction can be formed between the ZnO and the TiO₂, or even whether a tight contact can be established between the ZnO and the TiO₂. This is because when a close

^aSchool of Physics and Technology, and MOE Key Laboratory of Artificial Micro- and Nano-structures, Wuhan University, Wuhan 430072, China. E-mail: cxpan@whu.edu.cn; Tel: +86-027-68752481 ext. 8168

^bCenter for Electron Microscopy, Wuhan University, Wuhan 430072, China

connection and tight contact are formed at the interface between ZnO and TiO₂, the heterojunction will ensure the smooth transmission of photo-generated carriers, as well as adjusting their band structure and improving the physical and chemical properties. In this way, the long-term stability of the composite is guaranteed. However, this tight contact heterojunction is difficult to form *via* regular chemical methods at low temperatures, except by using epitaxial growth. In general, there exists only a mechanical contact at the interface which has many “gaps”, resulting in problems with stability and service life during long-term usage.

Generally, semiconductor photocatalysts can be divided into two groups, *i.e.*, powder suspensions and thin-films. Powders have advantages including large surface area, full contact with the degradable substances, full light acceptance and a higher photocatalytic efficiency, *etc.* However, they also have problems, such as needing to be stirred during the reaction and the difficulty of separating them out after the reaction.²² Recently, TiO₂ films have been paid much attention as useful photocatalysts for potential industrial applications.^{22,23} The main methods to prepare TiO₂ thin films include sol-gel methods,²⁴ magnetron sputtering,²⁵ and anodic oxidation,²⁶ as well as micro-arc oxidation (MAO).^{23,27,28}

MAO is a simple, economic and efficient technique for preparing a metal oxide film *in situ* upon the surface of valve metal, involving Al, Ti, Mg and their alloys. Oxide films produced by MAO exhibit many desired properties, such as good adhesion to substrates, high abrasibility, excellent chemical durability and high temperature resistance, *etc.*²⁷ It has been recognized that the surface morphology, thickness and phase structures of TiO₂ films grown upon Ti substrates *via* MAO can be simply adjusted through the experimental parameters, such as electrical parameters, and electrolyte components, to improve their properties.^{27,28}

In this paper, a novel ZnO/TiO₂ heterojunction composite with ZnO nanoneedles vertically grown on a TiO₂ film was prepared using a three-step process, *i.e.*, MAO, pulse plating and thermal oxidation. This composite film showed a prominent improvement in its photocatalytic properties. The reason was that in addition to having close contact with the substrate, an efficient and closely connected heterojunction was formed at the interface between the ZnO nanoneedles and the TiO₂ film during the high temperature thermal oxidation, which provided energy for atomic interdiffusion at the interface. This composite is also expected to have a good stability during long-term service.

2. Experimental section

Preparation of the TiO₂ film *via* MAO

A titanium alloy (Ti₆Al₄V) with a size of 1 cm × 1 cm × 0.6 cm was used as an anode. A stainless steel container was selected as an electrolyte cell as well as a cathode. The electrolyte solution was 10 g L⁻¹ analytical-grade Na₃PO₄, and high voltage power was used as a current supplier. During the 5 minutes of MAO treatment, the forward voltage was 550 V, the reverse voltage was 0 V, the frequency was 1200 Hz, and the duty cycle was 40%.

The temperature of the electrolyte was maintained by a condensate at below 25°.

Preparation of the ZnO/TiO₂ composite

A Zn nanocrystalline layer was deposited upon the surface of the TiO₂ film using square wave pulse plating. Standard Zn foil was selected as the anode, and the TiO₂ film as the cathode. During pulse plating, the forward voltage was 3.0 V, the reverse voltage was 1.0 V, and the duty cycle was 40%.^{12,20} Then a ZnO/TiO₂ heterojunction composite was obtained through the thermal oxidation of the Zn layer at 380 °C for 4 hours.

The crystalline structure of the ZnO/TiO₂ composite was characterized using an X-ray diffraction (XRD) spectrometer (D8 Advanced XRD; Bruker AXS, Karlsruhe, Germany) with CuK α radiation. The morphologies of the composites were observed using scanning electron microscopy (SEM) (S-4800, Hitachi High-Technologies Corporation Japan). Field emission gun scanning electron microscopy (FEG-SEM) (Sirion SEM, FEI, Netherlands) with an energy-dispersive X-ray spectrometer (EDS) was employed to characterize the chemical compositions. UV-vis diffuse reflectance spectra (DRS) of the composites were measured using the diffuse reflectance accessory of an ultraviolet-visible (UV-vis) spectrophotometer (UV-2550, Shimadzu, Kyoto, Japan).

Photogenerated current test

The prepared samples, a saturation calomel electrode and a platinum electrode were used as the working electrode, reference electrode and counter electrode, respectively. They were all immersed in 1 M Na₂SO₄ aqueous solution together. The working electrode of 1 cm² TiO₂ film was irradiated horizontally by a 160 W high pressure mercury lamp, which generated a light wavelength in the range of 350–450 nm. The distance between the lamp and electrode was 10 cm. The intensity of the photo-generated current was measured by an electrochemical workstation (CHI660C, Chenhua, Shanghai, China).

Photocatalytic deposition test

The photocatalytic activity of the ZnO/TiO₂ composites was measured by detecting the amount of ·OH generation, which was done according to the literature.^{28,36,37} The prepared samples were entirely immersed in a 2 mL aqueous solution containing 10 mM NaOH and 3 mM terephthalic acid (TA). Before exposure to the visible light irradiation, the solution was kept in the dark for 30 minutes. The samples were then irradiated perpendicularly by a 450 W high pressure mercury lamp. The fluorescence signal of the 2-hydroxy terephthalic acid was measured *in situ* every hour using a fluorescence spectrophotometer (F-4500, Hitachi, Japan). The excitation light employed in recording the fluorescence spectra was 320 nm. In the degradation experiments of methylene blue and methyl blue, the samples were immersed in a 3 mL solution with a concentration of 12 mg L⁻¹. The change of the solution concentration with the extension of irradiation time was measured by an UV-vis spectrophotometer.

3. Results and discussion

ZnO/TiO₂ composites were prepared according to three processes, *i.e.*, firstly, a TiO₂ layer was prepared as the substrate using MAO; then a Zn thin film was deposited upon the TiO₂ layer by pulse plating; and lastly, the composite Zn/TiO₂ was thermally oxidized in a regular furnace to cause a phase transformation from Zn into the ZnO nanoneedles. Fig. 1 illustrates the XRD patterns of the composite's phase structures at different stages. It can be seen that: (1) an anatase TiO₂ layer was formed on the surface of a titanium plate from MAO; (2) after the pulse plating, both Zn and TiO₂ diffraction peaks were indexed; (3) after thermal oxidation for four hours, both ZnO and TiO₂ peaks were observed, which indicated that the previous Zn film had been transformed into a ZnO phase, and the TiO₂ was still unchanged as anatase.

Fig. 2 shows the typical surface morphology of the TiO₂ layer formed by MAO, with craters. After a thin Zn film was deposited upon the TiO₂, the porous microstructures were still observed, as shown in Fig. 3. Fig. 4 shows the morphology of the dense ZnO nano-needles grown upon the TiO₂ surface after thermal oxidation. Fig. 5 shows elemental mappings for the ZnO/TiO₂ composite, which contained oxygen (O), titanium (Ti) and Zinc (Zn). Clearly, Zn atoms were relatively well distributed in the sample.

In our previous work, a lot of research was done on preparing ZnO nanoneedles by thermal oxidation,³⁸ which produced a kind of one-dimensional nanowire with a large root diameter (about 50 nm) and a small tip diameter (about 10 nm). The growth of the nanoneedles was supposed to be a kind of "solid state based-up diffusion model", which was different from the well-known V-L-S or V-S mechanisms. That is, driven by a contact electrical field between the Zn and ZnO interface, the Zn²⁺ on the (0001) plane diffused along the (0001) direction and generated ZnO with O²⁻ in the air, and at last a ZnO nanoneedle was formed. The Zn nanocrystalline plating and ZnO piezoelectric properties played key roles in the flourishing growth of the ZnO nanoneedles in the process.

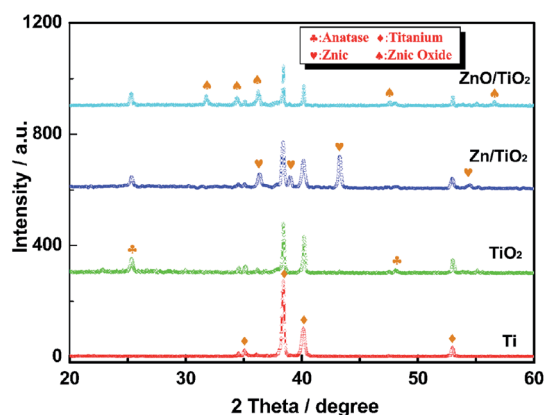


Fig. 1 X-ray diffraction patterns for the Ti substrate, TiO₂ and ZnO/TiO₂ heterojunction composite.

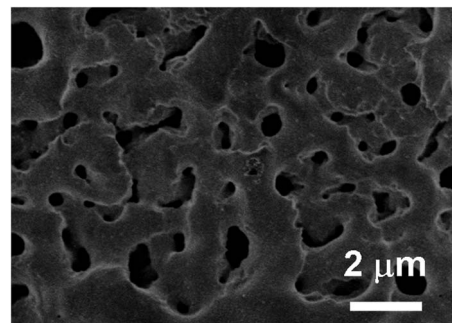


Fig. 2 SEM image showing the morphology of the original MAO TiO₂ film.

In the present work, the phase transformation from the Zn film to the ZnO nanoneedles happened on the TiO₂ surface during thermal oxidation (that is to say, the ZnO nanoneedles grew directly from the TiO₂ layer), and therefore, not only was a strong heterogeneous interface formed between the ZnO and the TiO₂, but it was also further strengthened due to the short-range interdiffusion of elements at the interface.¹² We believe that the interface prepared *via* thermal oxidation will eventually improve the electron movements between the ZnO and the TiO₂, and thus enhance the photocurrent performance of the composites.

In general, transmission electron microscopy (TEM) or high-resolution transmission electron microscopy (HRTEM) are ideal techniques for characterizing the interface between the ZnO and TiO₂. However, we found that it was nearly impossible to prepare a desired TEM specimen, because the TiO₂ layer prepared *via* MAO was tightly coupled with the titanium substrate. That was to say, during ultrasonic dispersion for TEM specimen preparation, the TiO₂ layer could not be separated from the substrate, while the ZnO nanoneedles were easily broken. Fig. 6 shows the SEM morphologies of the ZnO/TiO₂ composite after ultrasonic dispersion. Compared with Fig. 4, most of the ZnO nanoneedles had broken and washed off, as shown in Fig. 6(a), but their roots were still coupled with the TiO₂ layer, as shown in Fig. 6(b), which revealed a tight contact at the interface, and also exhibited a good stabilization.

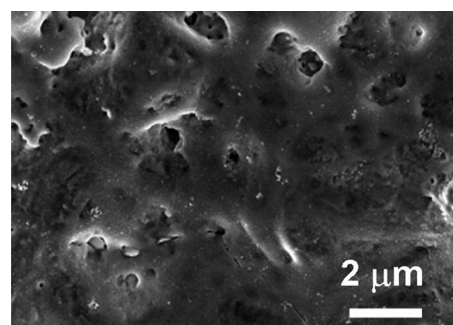


Fig. 3 SEM image showing the morphology of the MAO TiO₂ film covered with a Zn film.

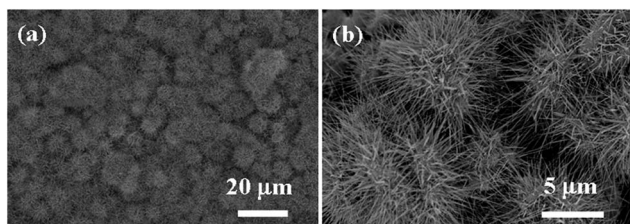


Fig. 4 SEM images showing the morphology of the ZnO/TiO₂ heterojunction composite with a nanoneedle-on-film structure: (a) low magnification; (b) high magnification.

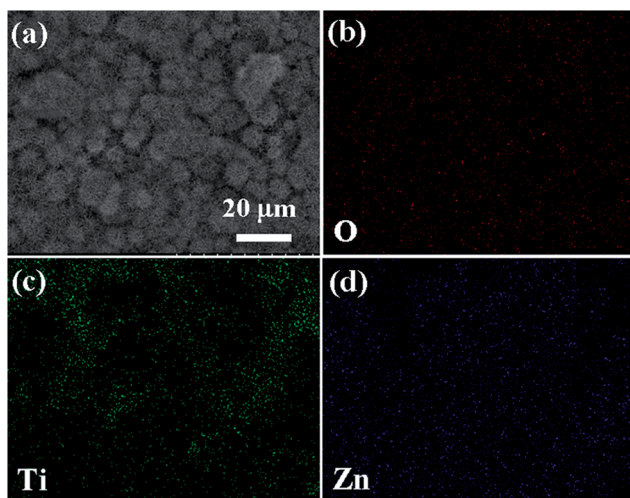


Fig. 5 (a) SEM image of the ZnO/TiO₂ heterojunction composite with a nanoneedle-on-film structure and the corresponding elemental maps: (b) oxygen at K peak, (c) Ti at K peak, (d) Zn at K peak.

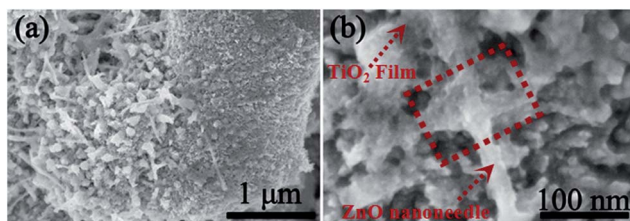


Fig. 6 SEM morphologies of the ZnO/TiO₂ composite with a nanoneedle-on-film structure after ultrasonic dispersion: (a) low magnification; (b) high magnification.

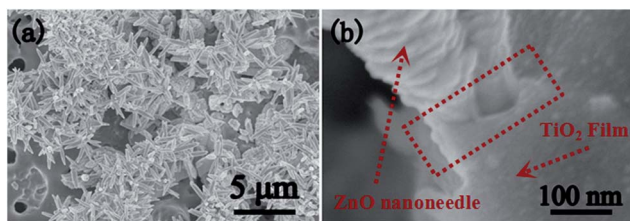


Fig. 7 SEM morphologies of the ZnO/TiO₂ composite with a nanoneedle-on-film structure after decreasing the pulse deposition time: (a) low magnification; (b) interface between ZnO and TiO₂.

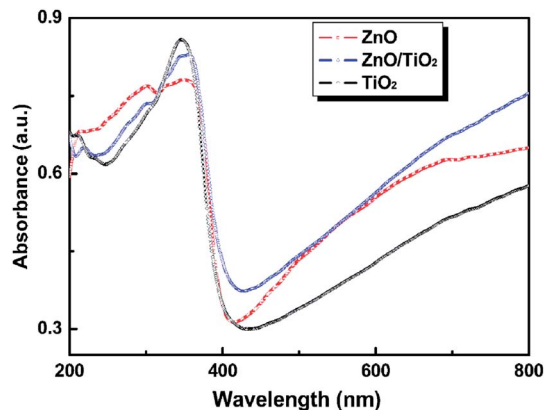


Fig. 8 UV-vis spectra of ZnO, TiO₂ and the ZnO/TiO₂ heterojunction composite.

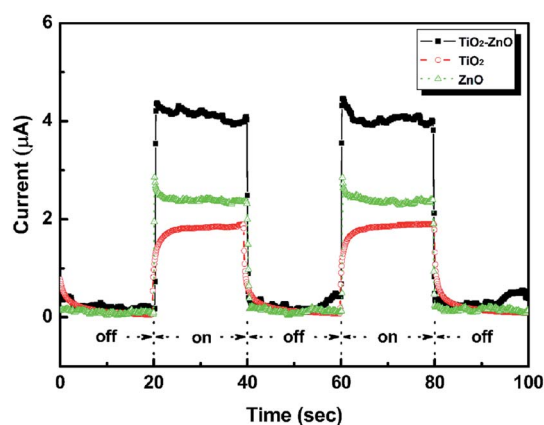


Fig. 9 Photogenerated current of the TiO₂, ZnO and ZnO/TiO₂ heterojunction composite.

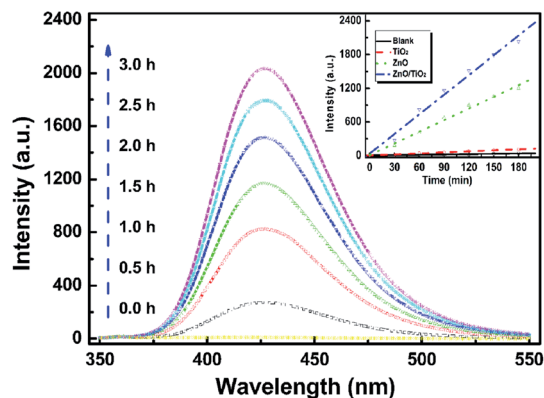


Fig. 10 Fluorescence spectra obtained for the supernatant liquid of the irradiated ZnO/TiO₂ solution containing 3 mM TA at various irradiation periods. The inset shows the time dependence of the fluorescence intensity at 426 nm of the TiO₂, ZnO and ZnO/TiO₂ composite.

In addition, in order to directly observe the interface, a new set of ZnO/TiO₂ composites was prepared with a short Zn deposition time of only 10 seconds, as shown in Fig. 7. In this

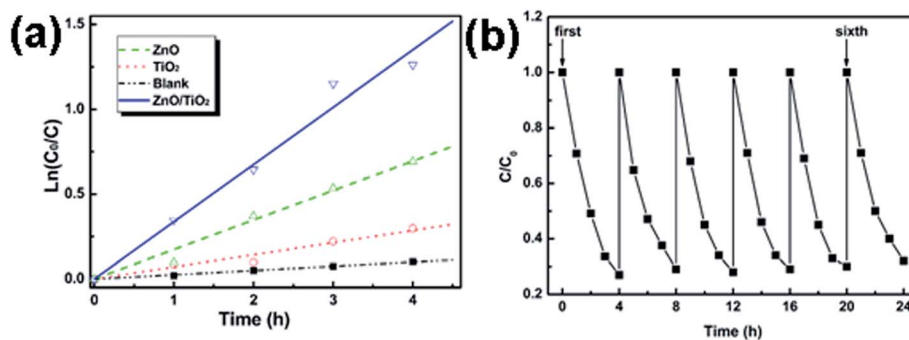


Fig. 11 (a) Relationship between $\ln(C_0/C)$ and the reaction time of methyl blue photocatalytic decomposition with the as-prepared photocatalysts of TiO₂, ZnO and the ZnO/TiO₂ composite; (b) cycle degradation of methyl blue with the ZnO/TiO₂ composite for 6 reuses.

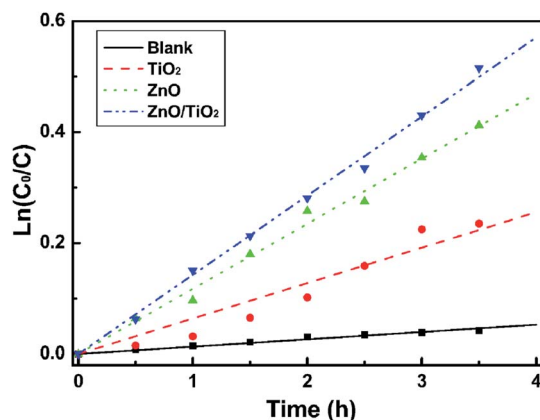


Fig. 12 Relationship between $\ln(C_0/C)$ and the reaction time of methylene blue photocatalytic decomposition with the as-prepared photocatalysts of TiO₂, ZnO and the ZnO/TiO₂ composite.

case, with a short pulse deposition time, the number of ZnO nanoneedles reduced greatly and the diameter became bigger, which provided a wide sphere of vision to directly observe the interface between the ZnO and the TiO₂, as shown in Fig. 7(b).

Fig. 8 illustrates the UV-vis absorption spectra of the samples. The ZnO used for reference was prepared by square wave pulse plating a Zn layer upon the surface of a titanium substrate, and then using thermal oxidation of the Zn layer at 380 °C for 4 hours. The strong absorption in the visible range of all samples was caused by the titanium substrate and has no contribution to the generation of electrons and holes.^{22,27} Regardless of the effect of the substrate, the experimental results revealed that the ZnO/TiO₂ composite exhibited a strong absorption for UV-vis light, when compared to pure ZnO and TiO₂. This is expected to have a positive impact on enhancing its photocatalytic properties.

In general, the photogenerated current test is an effective method for characterizing the electron-hole separation efficiency of semiconductors, which is associated with the intensity of illuminating light, chemical compositions and microstructures of photocatalysts. Fig. 9 illustrates the photogenerated current intensities of pure TiO₂, ZnO and the ZnO/TiO₂ composite irradiated by a high pressure mercury lamp under

the same conditions. Obviously, compared with the pure ZnO and TiO₂ layers, the current intensity of the ZnO/TiO₂ composite was improved significantly, indicating a high separation efficiency of the photo-generated carriers. This result could be ascribed to the tight contact heterojunction formed between the ZnO and the TiO₂, which was predicted to cause a significant improvement to the composite's photocatalytic effect.

It is well-known that the photocatalytic efficiency of catalysts can be effectively characterized by detecting the amount of $\cdot\text{OH}$ generation with irradiation. TA was used as the fluorescence probe because it can react with $\cdot\text{OH}$ in solution to generate 2-hydroxy terephthalic acid (TAOH), which emits a unique fluorescence signal at 426 nm.^{28,36,37} According to the literature,³⁶ during the photocatalytic process, TA only reacts with $\cdot\text{OH}$, generating TAOH, and so this was used as a fluorescence probe. Since the fluorescence intensity increased almost linearly with the irradiation time, the TAOH formation rate was calculated from this slope, which could evaluate the photocatalytic activity of the as-prepared samples. The fluorescence spectra associated with TAOH were generated by irradiating the ZnO/TiO₂ composite, as shown in Fig. 10. The inset of Fig. 10 is the time dependence of the fluorescence intensity at 426 nm of the TiO₂, ZnO and ZnO/TiO₂ composite. The results demonstrated that after photo-degradation for three hours, the photocatalytic efficiency of the ZnO/TiO₂ composite increased approximately two or three times more than that of pure TiO₂ and ZnO.

It is well established that the photocatalytic degradation of an organic dye is classified as exhibiting first-order kinetics, defined by the following equation:^{39,40}

$$\ln(C_0/C) = kt$$

where C_0 and C are the reactant concentration at times $t = 0$ and $t = t$, respectively, and k and t are the apparent reaction rate constant and time. A plot of $\ln(C_0/C)$ versus t will yield a slope of k .

The relationships between $\ln(C_0/C)$ and the reaction time are illustrated in Fig. 11(a) and Fig. 12. A linear behavior was observed for the samples and the results obeyed this kinetics. According to Fig. 11(a), the reaction rate constants of the three samples were $k(\text{ZnO}) = 0.17383 \text{ h}^{-1}$, $k(\text{TiO}_2) = 0.07141 \text{ h}^{-1}$, and $k(\text{ZnO/TiO}_2) = 0.3775 \text{ h}^{-1}$, respectively. The photocatalytic

efficiency of the ZnO/TiO₂ composites was improved 2.17 times more than that of the pure ZnO, and 5.29 times more than that of the pure TiO₂ film. Cycle degradation of methyl blue with the ZnO/TiO₂ composite was conducted, as shown in Fig. 11(b). Obviously, there was no decrease after recycling the composite 6 times, which proved there was a good stability of contact at the interface between the ZnO and the TiO₂. Similarly, the degradation of methylene blue also greatly improved with the data $k(\text{ZnO}) = 0.05868 \text{ h}^{-1}$, $k(\text{TiO}_2) = 0.03194 \text{ h}^{-1}$, $k(\text{ZnO/TiO}_2) = 0.07132 \text{ h}^{-1}$, as shown in Fig. 12.

We believe that the above results were due to the synergistic effect of TiO₂ and ZnO, which increased the separation efficiency of the photo-generated carriers, and thus improved the photocatalytic efficiency.³⁰ That is to say, the higher photocatalytic activity of the TiO₂/ZnO composite was related to the role of the ZnO nanoneedles grown upon the TiO₂ layer. According to our previous work, during high-temperature thermal oxidation, the Zn film was oxidized into ZnO nanoneedles, and there was good lattice matching between the TiO₂ and the ZnO through the short atom diffusion at the interface.^{12,20,21} Different to the relatively "loose" heterojunction prepared from regular chemical methods, this kind of tight contact heterojunction exhibited a great effect on the photo-generated carriers' movement.

According to the photocatalytic mechanism, under light irradiation, due to the energy band differences between the ZnO and the TiO₂, the photo-induced electrons will transfer from the ZnO conduction band to the TiO₂ conduction band, while the photo-induced holes move from the TiO₂ valence band to the ZnO valence band.^{12,30,36} During these transforming processes, we believe that the tight and compact heterojunction interface between the ZnO nanoneedles and the TiO₂ layer played a key role as a charge transport bridge, which significantly increased the separation efficiency of the photo-generated carriers, and enhanced the photocatalytic efficiency of the ZnO/TiO₂ composite.

4. Conclusions

A novel ZnO/TiO₂ heterojunction composite with a nanoneedle-on-film structure was prepared *via* three steps of MAO, plating and thermal oxidation. By using a high temperature treatment in air, metal Zn was directly transformed into ZnO nanoneedles upon the MAO TiO₂ layer, which formed a tight contact heterojunction between the ZnO and the TiO₂. This greatly increased the separation efficiency of the photo-induced carriers for improving the photocatalytic properties. This physical process provided an effective method for preparing high-performance thin-film photocatalysts. It exhibited several advantages, such as simplicity, economy, suitability for mass production, and potential applicability in the fields of photocatalysis, solar cells and supercapacitors, *etc.*

Acknowledgements

This research was supported by the National Natural Science Foundation of China (nos 11174227, 51209023, J1210061), the

Hubei Province Science and Technology Support Project (no. 2013BHE012), and the Fundamental Research Funds for the Central Universities.

Notes and references

- 1 A. Fujishima, X. T. Zhang and D. A. Tryk, *Surf. Sci. Rep.*, 2008, **63**, 515–582.
- 2 G. Liu, L. Z. Wang, H. G. Yang, H. M. Cheng and G. Q. Lu, *J. Mater. Chem.*, 2010, **20**, 831–843.
- 3 S. H. Nam, H. S. Shim, Y. S. Kim, M. A. Dar, J. G. Kim and W. B. Kim, *ACS Appl. Mater. Interfaces*, 2010, **2**, 2046–2052.
- 4 P. S. Archana, R. Jose, T. M. Jin, C. Vijila, M. M. Yusoff and S. Ramakrishna, *J. Am. Ceram. Soc.*, 2010, **93**, 4096–4102.
- 5 Y. P. Zhang, C. Z. Li and C. X. Pan, *J. Am. Ceram. Soc.*, 2012, **95**, 2951–2956.
- 6 R. Ostermann, D. Li, Y. D. Yin, J. T. McCann and Y. N. Xia, *Nano Lett.*, 2006, **6**, 1297–1302.
- 7 Z. Y. Liu, D. Sun, P. Guo and J. O. Leckie, *Nano Lett.*, 2007, **7**, 1081–1085.
- 8 M. A. Kanjwal, N. Barakat, F. A. Sheikh and H. Y. Kim, *J. Mater. Sci.*, 2010, **45**, 1272–1279.
- 9 D. L. Li and C. X. Pan, *Prog. Nat. Sci.*, 2012, **22**, 59–63.
- 10 Y. P. Zhang, L. F. Fei, X. D. Jiang, C. X. Pan and Y. Wang, *J. Am. Ceram. Soc.*, 2011, **94**, 4157–4161.
- 11 H. Y. Wang, Y. Yang, X. A. Li, L. J. Li and C. Wang, *Chin. Chem. Lett.*, 2010, **21**, 1119–1123.
- 12 D. L. Li, X. D. Jiang, Y. P. Zhang, B. Zhang and C. X. Pan, *J. Mater. Res.*, 2013, **28**, 507–512.
- 13 N. X. Wang, C. H. Sun, Y. Zhao, S. Y. Zhou, P. Chen and L. Jiang, *J. Mater. Chem.*, 2008, **18**, 3909–3911.
- 14 R. L. Liu, H. Y. Ye, X. P. Xiong and H. Q. Liu, *Mater. Chem. Phys.*, 2010, **121**, 432–439.
- 15 Y. X. Liu, Y. Z. Xie, J. T. Chen, J. Liu, C. T. Gao, C. Yun, B. G. Lu and E. Q. Xie, *J. Am. Ceram. Soc.*, 2011, **94**, 4387–4390.
- 16 M. A. Kanjwal, N. Barakat, F. A. Sheikh, S. J. Park and H. Y. Kim, *Macromol. Res.*, 2010, **18**, 233–240.
- 17 M. E. Fragala, I. Cacciotti, Y. Aleeva, R. Lo Nigro, A. Bianco, G. Malandrino, C. Spinella, G. Pezzotti and G. Gusmano, *CrystEngComm*, 2010, **12**, 3858–3865.
- 18 Y. Z. Li, W. Xie, X. L. Hu, G. F. Shen, X. Zhou, Y. Xiang, X. J. Zhao and P. F. Fang, *Langmuir*, 2010, **26**, 591–597.
- 19 A. B. Djuricic, X. Y. Chen, Y. H. Leung and A. Ng, *J. Mater. Chem.*, 2012, **22**, 6526–6535.
- 20 D. L. Li, W. H. Wu, Y. P. Zhang, L. L. Liu and C. X. Pan, *J. Mater. Sci.*, 2014, **49**, 1854–1860.
- 21 C. Z. Luo, D. L. Li, W. H. Wu, Y. P. Zhang and C. X. Pan, *RSC Adv.*, 2014, **4**, 3090–3095.
- 22 Y. Q. Wang, X. D. Jiang and C. X. Pan, *J. Alloys Compd.*, 2012, **538**, 16–20.
- 23 Y. Han, D. H. Chen and L. Zhang, *Nanotechnology*, 2008, **19**, 335705.
- 24 K. Y. Jung and S. B. Park, *Appl. Catal., B*, 2000, **25**, 249–256.
- 25 B. S. Liu, L. P. Wen and X. J. Zhao, *Sol. Energy Mater. Sol. Cells*, 2008, **92**, 1–10.
- 26 H. Yang and C. X. Pan, *J. Alloys Compd.*, 2010, **492**, L33–L35.

- 27 X. D. Jiang, Y. Q. Wang and C. X. Pan, *J. Alloys Compd.*, 2011, **509**, L137–L141.
- 28 X. D. Jiang, A. Q. Shi, Y. Q. Wang, Y. Z. Li and C. X. Pan, *Nanoscale*, 2011, **3**, 3573–3577.
- 29 N. Wang, X. Y. Li, Y. X. Wang, Y. Hou, X. J. Zou and G. H. Chen, *Mater. Lett.*, 2008, **62**, 3691–3693.
- 30 G. Marci, V. Augugliaro, M. J. Lopez-Munoz, C. Martin, L. Palmisano, V. Rives, M. Schiavello, R. Tilley and A. M. Venezia, *J. Phys. Chem. B*, 2001, **105**, 1033–1040.
- 31 D. W. Kim, S. Lee, H. S. Jung, J. Y. Kim, H. Shin and K. S. Hong, *Int. J. Hydrogen Energy*, 2007, **32**, 3137–3140.
- 32 Z. H. Zhang, Y. Yuan, Y. J. Fang, L. H. Liang, H. C. Ding and L. T. Jin, *Talanta*, 2007, **73**, 523–528.
- 33 L. Zhao, M. S. Xia, Y. H. Liu, B. J. Zheng, Q. Jiang and J. S. Lian, *J. Cryst. Growth*, 2012, **344**, 1–5.
- 34 J. T. Tian, L. J. Chen, Y. S. Yin, X. Wang, J. H. Dai, Z. B. Zhu, X. Y. Liu and P. W. Wu, *Surf. Coat. Technol.*, 2009, **204**, 205–214.
- 35 R. S. Mane, W. J. Lee, H. M. Pathan and S. H. Han, *J. Phys. Chem. B*, 2005, **109**, 24254–24259.
- 36 T. Hirakawa and Y. Nosaka, *Langmuir*, 2002, **18**, 3247–3254.
- 37 W. Xie, Y. Z. Li, W. Sun, J. C. Huang, H. Xie and X. J. Zhao, *J. Photochem. Photobiol., A*, 2010, **216**, 149–155.
- 38 W. Yu and C. X. Pan, *Mater. Chem. Phys.*, 2009, **115**, 74–79.
- 39 I. K. Konstantinou and T. A. Albanis, *Appl. Catal., B*, 2004, **49**, 1–14.
- 40 D. L. Liao, C. A. Badour and B. Q. Liao, *J. Photochem. Photobiol., A*, 2008, **194**, 11–19.